Journal of Anatomy

J. Anat. (2020) **236**, pp98–104 doi: 10.1111/joa.13088

Reduction of olfactory and respiratory turbinates in the transition of whales from land to sea: the semiaquatic middle Eocene *Aegyptocetus tarfa*

Emanuele Peri,[1] Philip D. Gingerich,[2] Giacomo Aringhieri[3] and Giovanni Bianucci[1]

[1]*Dipartimento di Scienze della Terra, Università di Pisa, Pisa, Italy*
[2]*Museum of Paleontology, University of Michigan, Ann Arbor, MI, USA*
[3]*Diagnostic and Interventional Radiology, Department of Translational Research and New Technologies in Medicine and Surgery, University of Pisa, Pisa, Italy*

Abstract

Ethmoturbinates, nasoturbinates, and maxilloturbinates are well developed in the narial tract of land-dwelling artiodactyls ancestral to whales, but these are greatly reduced or lost entirely in modern whales. *Aegyptocetus tarfa* is a semiaquatic protocetid from the middle Eocene of Egypt. Computed axial tomography scans of the skull show that *A. tarfa* retained all three sets of turbinates like a land mammal. It is intermediate between terrestrial artiodactyls and aquatic whales in reduction of the turbinates. Ethmoturbinates in *A. tarfa* have 26% of the surface area expected for an artiodactyl. These have an olfactory function and indicate that early whales retained a sense of smell in the transition from land to sea. Maxilloturbinates in *A. tarfa* have 6% of the surface area expected for an artiodactyl. These have a respiratory function and their markedly reduced size suggests that rapid inhalation and exhalation was already more important than warming and humidifying air, in contrast to extant land mammals. Finally, the maxilloturbinates of *A. tarfa*, although greatly reduced, still show some degree of similarity to those of artiodactyls, supporting the phylogenetic affinity of cetaceans and artiodactyls based on morphological and molecular evidence.

Key words: Archaeoceti; Artiodactyla; computed axial tomography scans; Eocene; Protocetidae; turbinates.

Introduction

The nasal chamber of mammals typically contains three sets of epithelium-covered bony plates, or turbinates. Posterior turbinates associated with the ethmoid bones, the ethmoturbinates, have an olfactory function (Van Valkenburgh et al. 2004, 2011; Pihlström, 2008). Anterior turbinates associated with the maxillary bones, the maxilloturbinates, have a respiratory function: they warm and humidify air as it is inspired, and recover heat and water from air as it is expired (Hillenius, 1992, 1994; Van Valkenburgh et al. 2004; Crompton et al. 2015). Dorsal turbinates associated with the nasal bones, the nasoturbinates, are located more centrally in the nasal cavity, above and behind the maxilloturbinates and above and in front of the ethmoturbinates. The function of the nasoturbinates is not fully understood, although it seems that they have a predominantly olfactory function (Hillenius 1992; Van Valkenburgh et al. 2004, 2011; Harkema et al. 2006).

Turbinates are present and important in almost all mammalian groups, but extant aquatic Cetacea are an exception. Modern odontocetes have no turbinates at all and modern mysticetes preserve only rudimentary ethmoturbinates (Godfrey et al. 2012; Godfrey 2013; Berta et al. 2014; Buono et al. 2015). The fossil record shows that whales evolved from terrestrial Artiodactyla (Gingerich et al. 2001; Thewissen et al. 2007; Uhen, 2010) and several genomic studies identify Hippopotamidae as the closest extant relatives of cetaceans (Geisler & Theodor, 2009; Zhou et al. 2011; Hassanin et al. 2012). Gatesy et al. (2013) analysed molecular and paleontological data and reinforced previous molecular studies by recognising *Hippopotamus* within Artiodactyla as the extant sister group of whales. Artiodactyls all have three sets of turbinates – ethmoid, nasal, and maxillary – well developed (Hillenius, 1992; Clifford & Witmer, 2004a,b), and turbinates were clearly reduced and lost as whales evolved to become fully aquatic (Berta et al. 2014).

Correspondence
Giovanni Bianucci, Dipartimento di Scienze della Terra, Università di Pisa, Pisa 56126, Italy. E: bianucci@dst.unipi.it

Accepted for publication *13 August 2019*
Article published online *9 September 2019*

Although the turbinates are thin, delicate bone structures that lie within the nasal cavity of a skull, making them difficult to see, they are preserved in some Eocene archaeocetes, the stem group for cetaceans. The first description of turbinates in an archaeocete was by Stromer (1903) in the late Eocene basilosaurid *Saghacetus osiris*. Ethmoturbinates are preserved in Stromer's specimen as delicate laminae of bone encased in fine sediment filling the nasal capsule. Uhen (2004) observed similarly preserved ethmoturbinates forming a bony labyrinth in another late Eocene basilosaurid, *Dorudon atrox*, where the ethmoturbinates extend as far anteriorly as the mesethmoid supporting them. Ethmoturbinates were identified in a specimen attributed to the middle Eocene remingtonocetid *Andrewsiphius* sp. (Pihlström, 2008; Thewissen & Nummela, 2008) and a ridge for possible attachment of maxilloturbinates was identified in *Remingtonocetus* (Bajpai et al. 2011). Ethmoturbinates have also been reported in the middle Eocene protocetids *Artiocetus clavis* (Fahlke et al. 2011), *Aegyptocetus tarfa* (Bianucci & Gingerich, 2011), and a protocetid of unknown genus and species (Godfrey et al. 2012). Neither nasoturbinates nor maxilloturbinates were observed in these specimens.

The purpose of this study is to reconstruct the three-dimensional size and shape of turbinates in the nasal cavity of the holotype of *A. tarfa* and to comment on their function and stage of reduction relative to artiodactyls as land mammals and to extant cetaceans as fully aquatic mammals. The holotype of *A. tarfa* is exceptionally well preserved. It was found in fine-grained marbleized limestone from the middle Eocene of Egypt after it was exported commercially to Italy, where the limestone was cut into slabs of decorative facing stone, revealing the fossil. The specimen, a partial skeleton, is preserved in the Museo di Storia Naturale dell'Università di Pisa (MSNUP). Bianucci & Gingerich (2011) described ethmoturbinates visible on the surface of one of the limestone slabs. Here we use computerized axial tomography (CT) to study the full set of turbinates in *A. tarfa*. Nasoturbinates and maxilloturbinates are present in *A. tarfa* in addition to ethmoturbinates, which has enabled the first quantitative description of turbinate surface areas within an archaeocete and the first quantitative comparison with artiodactyls as representatives of the land-mammal ancestry of whales.

Materials and methods

We analysed the skull of the holotype of *Aegyptocetus tarfa* (MSNUP I15459) and, for comparison, skulls of the following five extant artiodactyls in the zoological collections of the MSNUP:

- *Alcelaphus buselaphus buselaphus* (Bovidae: African hartebeest) (MSNUP C1343)
- *Boselphus tragocamelus* (Bovidae: Indian nilgai) (MSNUP C1423)
- *Camelus dromedarius* (Camelidae: Arabian camel) (MSNUP C1435)
- *Hippopotamus amphibius* (Hippopotamidae: African hippopotamus) (MSNUP C228)
- *Sus scrofa* (Suidae: Eurasian wild pig) (MSNUP C1418)

Specimens were chosen to represent a range of shape and size variation from turbinates in skulls of artiodactyls comparable in size to *A. tarfa*. All skulls were CT-scanned in Azienda Ospedaliero-Universitaria di Pisa. The machine used was a GE LightSpeed RT 16, with a slice thickness of 1.25 mm and spacing between slices of 0.625 mm. CT-scans were analysed with open-access MANGO software for medical image visualization (Multi-image Analysis GUI; http://rii.uthscsa.edu/mango/). MANGO was also used to create virtual 3D models of turbinates and to calculate their surface area. The skull of *A. tarfa* is weakly asymmetrical due to its clockwise torsion (Bianucci & Gingerich, 2011), so turbinates were mapped on both sides. Artiodactyl skulls are bilaterally symmetrical, and mapping was confined to turbinates of the left side of the skull (Ranslow et al. 2014). Surface area measurements for artiodactyls were then doubled to represent both left and right sides.

There are two sources of uncertainty in measurements of the fossil *A. tarfa*. Differences in bone and sediment density enabled reconstruction of the three-dimensional shape of turbinates when surrounded by calcareous matrix, but the resolution was lower than for skulls of extant artiodactyls with empty nasal cavities. In addition, it was necessary to reconstruct turbinates damaged when the *A. tarfa* skull entombed in matrix was cut into slabs (Bianucci & Gingerich, 2011). Uncertainty of measurements in the extant artiodactyls was due to breakage of the thinnest laminae of bone. All these sources of uncertainty cause turbinate areas to be similarly underestimated, meaning comparisons should still be reliable within and between taxa.

The relative sizes of turbinates in *A. tarfa* were compared with those of artiodactyls in three ways. First, we compared the area of the ethmoturbinate surface (ETS), the area of the nasoturbinate surface (NTS), and the area of the maxilloturbinate surface (MTS) with the total turbinate surface (TTS). In the second comparison, we measured the size of the turbinate chamber surface (TCS) within the nasal chamber of *A. tarfa*. This measured value of TCS was then compared with TCS for an animal with the skull length, bizygomatic skull width, and bodyweight of *A. tarfa*, based on TCS measured in the five extant artiodactyls. Turbinates do not fill the whole nasal chamber. The anterior end of the turbinate chamber coincides with the anterior extremity of the maxilloturbinates, and its posterior end coincides with the ethmoidal portion of the cribriform plate (excluding the maxilla). In this comparison, the natural logarithm (ln) of the square root of TCS was regressed on ln cranial length (cm), on ln cranial width (cm), and on ln cube root of bodyweight (kg) for the artiodactyls. TCS was measured using the same methods as those described above for calculating the surface area of turbinates. Skull length and width were measured on the skulls used for CT scanning. The bodyweight for *A. tarfa* is that estimated by Bianucci & Gingerich (2011). Bodyweights for the artiodactyls were estimated from a regression of bodyweight on skull length (Janis, 1990).

Finally, we compared the surface area for each set of turbinates, ETS, NTS, and MTS, with the area expected, based on extant artiodactyl, for the set given the associated TCS. Measured values for ETS, NTS, and MTS in *A. tarfa* were compared with the values expected from regressions of artiodactyl ETS, NTS, and MTS on TCS.

Results

CT-scans show that the turbinate sets in Eocene *Aegyptocetus tarfa* are slightly asymmetrical (Fig. 1a,b). This feature is possibly related to the clockwise torsion of the rostrum (Bianucci & Gingerich, 2011), a genuine anatomical feature that has also been observed in other archaeocetes (Fahlke et al. 2011; Fahlke & Hampe, 2015). This hypothesis is supported by the fact that, in *A. tarfa*, the maxilloturbinates, which extend more anteriorly in the rostrum than ethmoturbinates and nasoturbinates, exhibit the greater degree of asymmetry (i.e. the right maxilloturbinates are slightly wider transversely than the left maxilloturbinates). The ethmoturbinates, like those in other mammals (Hillenius, 1994), are convoluted and densely packed in the olfactory recess. Left and right nasoturbinates are elongated, narrow, and, for most of their length, a single laterally concave lamina of bone. Posteriorly, a second medially concave plate appears, giving the nasoturbinates in this region a more tubular appearance. Left and right maxilloturbinates are small compared with those of modern artiodactyls (Fig. 1c–h), and the maxilloturbinates occupy a relatively small portion of the nasal chamber. They do not extend anteriorly beyond the nasoturbinates. Their morphology is simple: the most anterior part of the lamina is hook-shaped and concave dorsally and laterally (Fig. 2a). There is a narrow downward-facing lamina in the middle part, and the posterior part of the lamina is again hook-shaped.

Maxilloturbinates of *A. tarfa* and the five artiodactyls studied for comparison are illustrated in red in the cross-sections of skulls in Fig. 2. All of the artiodactyls have elongated, double (lower and upper) scroll-shaped maxilloturbinates without projecting branches (Fig. 2b–f). The upper scroll is more developed and convoluted than the lower scroll. These features, which have been observed in all specimens, are typical of and exclusive to artiodactyls (Hillenius, 1992). For example, the maxilloturbinates of *Equus caballus* (Perissodactyla) have a single high and narrow scroll; also, they show a greater thickness than the maxilloturbinates of artiodactyls (Arencibia et al. 2000: figures 7–8, where the maxilloturbinates are named 'ventral conchal bulla'). Carnivora have richly branching double-scroll-shaped maxilloturbinates (Van Valkenburgh et al. 2004).

The maxilloturbinates of *A. tarfa* clearly differ from those of carnivores in lacking the external branches, while they exhibit some affinities with those of artiodactyls. Indeed, the maxilloturbinates of *A. tarfa* could be considered a simplified version of the artiodactyl double scroll (Fig. 2a). The upper scroll in *A. tarfa* is reduced to only one half-round. The lower scroll has almost disappeared but there is a small branch at mid-length of the maxilloturbinates suggesting a lower scroll. Similarities to *Equus caballus* are weaker because the latter has the lower scroll completely missing (Arencibia et al. 2000).

Measurements for each set of turbinates are given in Table 1. When we compare the ETS, NTS, and MTS areas for artiodactyls with their sum, TTS, we find modal proportions of 0.42, 0.14, and 0.41, respectively. These proportions are 0.61, 0.20, and 0.15 in *A. tarfa*, indicating that *A. tarfa* has more of its turbinate area devoted to ethmoturbinates than expected from comparison with artiodactyls, and less devoted to maxilloturbinates.

We can compare turbinate size in a different way by asking how the area of TCS compares with body size measured by skull length, skull width or bodyweight. *A. tarfa* has a skull length of 68 cm (Table 1). Regression of ln $\sqrt{\text{TCS}}$ on skull length for artiodactyls (Fig. 3a) yields an expected TCS for *A. tarfa* of 195 604 mm^2, corresponding to ln square-root value of about 6.092. The observed TCS for *A. tarfa* is 64 953 mm^2, corresponding to ln square-root value of 5.541. Thus, the residual for length (observed minus expected) is calculated to be −0.549 and the corresponding proportion 0.333. In the previous paragraph, we noted that TCS of *A. tarfa* is about 33% as large as expected for an artiodactyl of the same skull length.

Similar calculations show that TCS for *A. tarfa* is about 57% as large as expected for an artiodactyl of the same skull width, and about 63% as large as expected for an artiodactyl of the same bodyweight. Variation in the residuals and proportions observed here are probably related to differences in skull shape for the species compared. Taking the median, we conclude that the area of TCS is about 57% as large as expected in an artiodactyl of the same size.

Another way to compare turbinate size is to compare the turbinate area observed in *A. tarfa* with the turbinate area expected for an artiodactyl of the same TCS. The comparison for ethmoturbinates is shown in Fig. 3b, where the observed-minus-expected residual for ln ETS is −0.76, and ETS itself is 0.47 the size expected for TCS observed in *A. tarfa*. Similar calculations for nasoturbinates and maxilloturbinates are shown in Fig. 3c–d, where the residuals are −0.78 and −2.30, respectively, and the corresponding proportions for NTS and MTS are 0.46 and 0.10 the size expected for TCS observed in *A. tarfa*. Combining all observations in Fig. 3 by multiplying each proportion in Fig. 3b–d by 0.566 from Fig. 3a, ETS and NTS for *A. tarfa* are each about 26% of the size expected for an artiodactyl, and MTS for *A. tarfa* is about 6% of the size expected for an artiodactyl.

Discussion

Morphofunctional considerations

The general trend of reduction of turbinate size from artiodactyls to extant cetaceans (Berta et al. 2014) is supported by three-dimensional reconstruction of the turbinates of *A. tarfa* and comparison of their size and shape with the turbinates of extant artiodactyls. Ethmoturbinates,

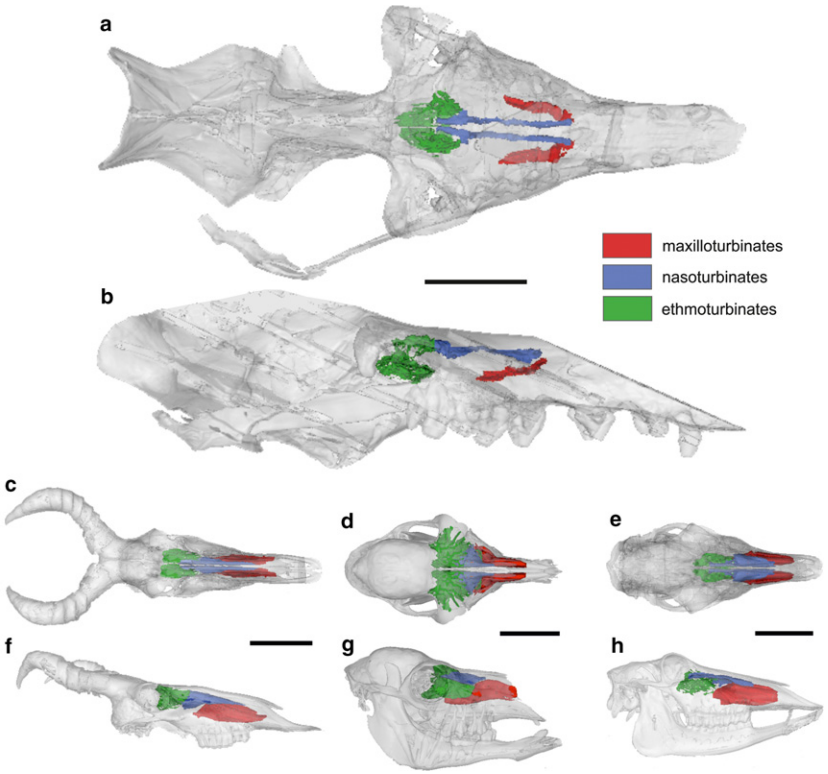

Fig. 1 Three-dimensional CT-scan reconstruction of skulls and related turbinates in dorsal and lateral view. (a,b) *Aegyptocetus tarfa*, MSNUP I15459. (c,d) *Alcelaphus buselaphus*, MSNUP C1343. (e,f) *Camelus dromedarius*, MSNUP C1435. (g,h) *Boselaphus tragocamelus*, MSNUP C1423. Scale bar: 10 cm.

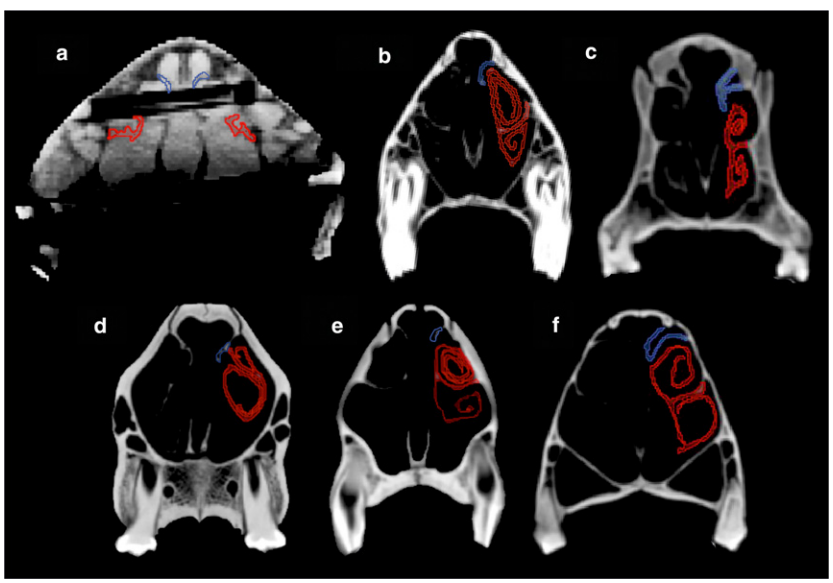

Fig. 2 Left and right maxilloturbinates (red) and nasoturbinates (blue) in CT-scan cross-sections of skulls studied here. (a) *Aegyptocetus tarfa*, MSNUP I15459. (b) *Alcelaphus buselaphus*, MSNUP C1343. (c) *Sus scrofa*, MSNUP C1418. (d) *Hippopotamus amphibious*, MSNUP C228. (e) *Camelus dromedarius*, MSNUP C1435. (f) *Boselaphus tragocamelus*, MSNUP C1423. All sections were taken at the anteroposterior midpoint of the maxilloturbinates and all sections are reduced to the same height. Note the small size and simple structure of maxilloturbinates in *A. tarfa* compared with those of artiodactyls.

Table 1 Measurements of body size, turbinate chamber surface area, and ethmoturbinate, nasoturbinate, and maxilloturbinate surface areas in comparative Artiodactyla and the middle Eocene archaeocete *Aegyptocetus tarfa*

Genus and species	Cranial length (cm)	Cranial width (cm)	Bodyweight (kg)	TCS (mm^2)	ETS (mm^2)	NTS (mm^2)	MTS (mm^2)	TTS (mm^2)	ETS/TTS	NTS/TTS	MTS/TTS
Artiodactyla											
Boselphus tragocamelus	38.0	15.4	227	63 813	25 262	12 532	53 745	91 540	0.28	0.14	0.59
Alcelaphus buselaphus	34.6	11.5	309	63 355	30 424	19 355	44 117	93 896	0.32	0.21	0.47
Hippopotamus amphibius	63.6	37.4	1532	177 606	114 138	32 039	102 397	248 574	0.46	0.13	0.41
Camelus dromedarius	34.0	15.0	260	51 298	55 753	11 232	42 677	109 662	0.51	0.10	0.39
Sus scofa	30.9	15.6	122	52 376	22 274	11 011	19 513	52 798	0.42	0.21	0.37
Median	**34.6**	**15.4**	**260**	**63 355**	**30 424**	**12 532**	**44 117**	**93 896**	**0.42**	**0.14**	**0.41**
Archaeoceti											
Aegyptocetus tarfa	**68.0**	**27.0**	**650**	**64 953**	**17 010**	**6638**	**4158**	**27 806**	**0.61**	**0.24**	**0.15**

Right-hand columns list ETS, NTS, and MTS as a proportion of TTS. Medians are in bold.

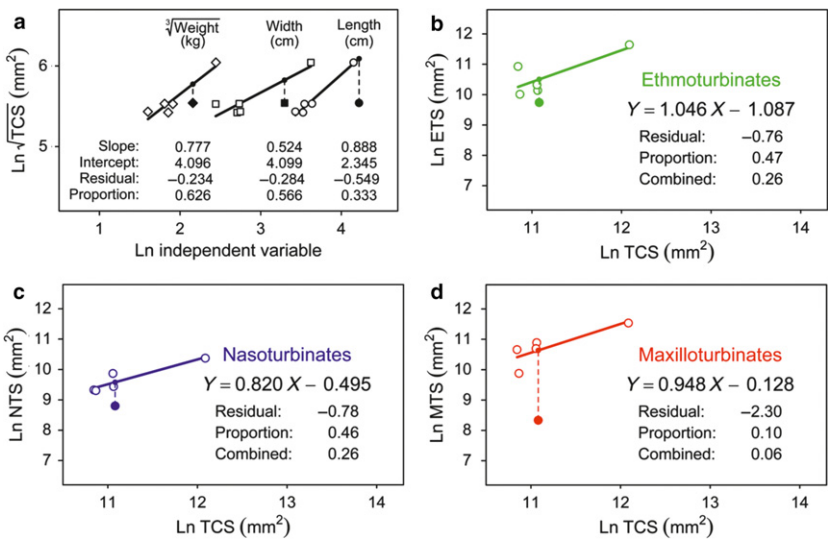

Fig. 3 Turbinate size observed in middle Eocene *Aegyptocetus tarfa* (solid symbols) compared with turbinate size in five species of extant artiodactyls (open symbols). (a) Allometric scaling of TCS with length, width, and the cube root of bodyweight. (b) Allometric scaling of ETS with TCS. (c) Allometric scaling of NTS with TCS. (d) Allometric scaling of MTS with TCS. Dashed lines are projections showing the distance between observation and expectation. 'Proportion' is the residual expressed as a ratio of observation to expectation. 'Combined' is the median proportion in (a) multiplied by the proportion in (b), (c), or (d). Measurements plotted here are listed in Table 1. (Online version in colour.)

nasoturbinates, and maxilloturbinates are all retained in *A. tarfa*, but are all reduced in size compared with expectation based on artiodactyls. As calculated above, ETS and NTS are each about 26% of the area expected for an artiodactyl, and MTS is about 6% of the expected size. This atrophy in *A. tarfa* cannot have been caused by postmortem breakage, because observations made on cross-sections of the skull before reassembly showed excellent preservation of the turbinates (Bianucci & Gingerich, 2011: figures 4–5). Further, three-dimensional reconstruction of the *A. tarfa* turbinates shows a close correspondence of turbinates on the left and right sides of the skull. Thus, we consider the turbinates of *A. tarfa*, to be complete (except for the parts destroyed by the cuts) and regard the reconstruction shown in Fig. 1a–b as reliable.

An ethmoturbinate and nasoturbinate reduction to 26% of expected value in *A. tarfa* is relatively easy to explain. Terrestrial mammals use olfaction to locate food and to communicate in social interactions (Hillenius, 1992, 1994; Van Valkenburgh et al. 2011). *A. tarfa* was a

semiaquatic predator, hunting in water like other protocetids (Gingerich, 2003; Bianucci & Gingerich, 2011). Mammalian olfactory receptors differ from those of fishes and amphibians and do not work well in water (Pihlström, 2012), so olfaction would have had limited use for locating prey. *A. tarfa*, like other protocetids, was considered able to hear high sonic frequencies, facilitating predation on sound-producing fish (Bianucci & Gingerich, 2011; Fahlke et al. 2011), although a recent study based on the cochlear morphology questioned specialization for ultrasonic hearing among archaeocetes (Mourlam & Orliac, 2017).

Reduction of ethmoturbinates is also observed in pinnipeds. Van Valkenburgh et al. (2011), citing Laska (2005), interpreted ethmoturbinate reduction in pinnipeds as reflecting a reduction in olfactory acuity, the range of smells that can be detected, but not olfactory sensitivity or discrimination within a narrower range. Based on this reasoning, *A. tarfa* was probably able to detect and distinguish a restricted range of smells when on land or on the sea surface. This would be important for mate identification and calf recognition.

Near complete atrophy of maxilloturbinates in *A. tarfa* is more difficult to explain. Maxilloturbinates play an important role in heat and water retention in modern mammals. Van Valkenburgh et al. (2011) found the surface area of ethmoidal or olfactory turbinates to be about three times greater than the surface area of maxillary or respiratory turbinates in terrestrial carnivores, and the opposite to be true in aquatic carnivores. Pinnipeds, with marine adaptations parallelling those of protocetids, have maxilloturbinates with a greater surface area than their ethmoturbinates (Van Valkenburgh et al. 2011), which is the opposite of what we see in comparing *A. tarfa* to artiodactyls or to terrestrial carnivores (Van Valkenburgh et al. 2011).

Modern cetaceans have a smooth-walled narial tract lacking respiratory turbinates, which Reidenberg & Laitman (2008) consider an advantage for rapid friction-free exchange of large volumes of air during brief breathing events at the sea surface. Rapid transfer of air during breathing may have been important for protocetids like *A. tarfa*. Middle Eocene oceans were 6–8 °C warmer than oceans today (Zachos, 2001) and the relatively constant humidity of an evaporative environment at the sea surface would reduce the need for both heat and water retention. The extreme reduction of maxilloturbinates could also be a consequence of the moderate posterior shift of the position of the external bony nares observed in *A. tarfa* and other protocetids. In fact, such a shift reduced the length of the nasal passage. The retention of reduced turbinates in some archaic odontocetes displaying limited telescopy and external bony nares that still do not reach the vertex of the skull (Churchill et al. 2018) lends some support to this hypothesis.

Phylogenetic considerations

The comparison of turbinate cross-sections in Fig. 2 shows that maxilloturbinates of *A. tarfa*, although greatly reduced, still show some similarity to those of artiodactyls, supporting the phylogenetic affinity of cetaceans and artiodactyls based on other evidence (Gingerich et al. 2001; Thewissen et al. 2007; Uhen, 2010). Morphological differences between the maxilloturbinates of cetaceans and artiodactyls (both having the typical double scroll morphology) compared with perissodactyls (with only an upper scroll) and carnivores (where branching turbinates replace scrolls) are consistent with the phylogenetic distance between these three mammalian clades.

Molecular analyses place Hippopotamidae, within extant Artiodactyla, as the closest living relative of Cetacea (Geisler & Theodor, 2009; Zhou et al. 2011; Hassanin et al. 2012; Gatesy et al. 2013), with the divergence time of hippos and cetaceans estimated at 52.4 Ma (Orliac et al. 2010). Maxilloturbinates of *Hippopotamus amphibius* are most similar to those of other artiodactyls and do not show any special similarity to maxilloturbinates of *A. tarfa* (Fig. 2). This is not surprising, considering the great reduction of maxilloturbinates in *A. tarfa*.

Acknowledgements

We thank Simone Farina and Chiara Sorbini for providing access to collections under their care, Davide Caramella and Davide Giustini for the CT scanning and for useful suggestions about the processing of CT-scan images, and Walter Landini for stimulating discussions.

Author contributions

E.P. and G.A. analysed and processed the CT-scan images. E.P., G.B., and P.D.G., wrote the paper. G.B. supervised the project. All authors discussed the paper and gave final approval for publication.

Conflict of interest

We declare we have no competing interests.

References

Arencibia A, Vazquez JM, Jaber R, et al. (2000) Magnetic resonance imaging and cross sectional anatomy of the normal equine sinuses and nasal passages. *Vet Radiol Ultrasound* **41**, 313–319.

Bajpai S, Thewissen JGM, Conley RW (2011) Cranial anatomy of middle Eocene *Remingtonocetus* (Cetacea, Mammalia) from Kutch, India. *J Paleontol* **85**, 703–718.

Berta A, Ekdale EG, Cranford TW (2014) Review of the cetacean nose: form, function, and evolution. *Anat Rec* **297**, 2205–2215.

Bianucci G, Gingerich PD (2011) *Aegyptocetus tarfa*, n. gen. et sp. (Mammalia, Cetacea), from the middle Eocene of Egypt:

clinorhynchy, olfaction, and hearing in a protocetid whale. *J Vert Paleontol* **31**, 1173–1188.

Buono MR, Fernández MS, Fordyce RE, et al. (2015) Anatomy of nasal complex in the southern right whale, *Eubalaena australis* (Cetacea, Mysticeti). *J Anat* **226**, 80–92.

Churchill M, Geisler JH, Beatty BL, et al. (2018) Evolution of cranial telescoping in echolocating whales (Cetacea: Odontoceti). *Evolution* **72**, 1092–1108.

Clifford AB, Witmer LM (2004a) Case studies in novel narial anatomy: 2. The enigmatic nose of moose (Artiodactyla: Cervidae: *Alces alces*). *J Zool* **262**, 339–360.

Clifford AB, Witmer LM (2004b) Case studies in novel narial anatomy: 3. Structure and function of the nasal cavity of saiga (Artiodactyla: Bovidae: *Saiga tatarica*). *J Zool* **264**, 217–230.

Crompton AW, Musinsky C, Owerkowicz T (2015) Evolution of the mammalian nose. In: *Great Transformations in Vertebrate Evolution* (eds Dial K, Shubin N, Brainerd E), pp. 189–203. Chicago: University of Chicago Press.

Fahlke JM, Hampe O (2015) Cranial symmetry in baleen whales (Cetacea, Mysticeti) and the occurrence of cranial asymmetry throughout cetacean evolution. *Sci Nat* **102**, 1–16.

Fahlke JM, Gingerich PD, Welsh RC, et al. (2011) Cranial asymmetry in Eocene archaeocete whales and the evolution of directional hearing in water. *PNAS* **108**, 14545–14548.

Gatesy J, Geisler JH, Chang J, et al. (2013) A phylogenetic blueprint for a modern whale. *Mol Phylogenet Evol* **66**, 479–506.

Geisler JH, Theodor JM (2009) Hippopotamus and whale phylogeny. *Nature* **458**, E1–E4.

Gingerich PD (2003) Land-to-sea transition in early whales: evolution of Eocene Archaeoceti (Cetacea) in relation to skeletal proportions and locomotion of living semiaquatic mammals. *Paleobiology* **29**, 429–454.

Gingerich PD, ul Haq M, Zalmout IS, et al. (2001) Origin of whales from early artiodactyls: hands and feet of eocene protocetidae from Pakistan. *Science* **293**, 2239–2242.

Godfrey SJ (2013) On the olfactory apparatus in the Miocene odontocete *Squalodon* sp. (Squalodontidae). *C R Palevol* **12**, 519–530.

Godfrey SJ, Geisler J, Fitzgerald EMG (2012) On the olfactory anatomy in an archaic whale (Protocetidae, Cetacea) and the minke whale *Balaenoptera acutorostrata* (Balaenopteridae, Cetacea). *Anat Rec* **296**, 257–272.

Harkema JR, Carey SA, Wagner JG (2006) The nose revisited: a brief review of the comparative structure, function, and toxicologic pathology of the nasal epithelium. *Toxicol Pathol* **34**, 252–269.

Hassanin A, Delsuc F, Ropiquet A, et al. (2012) Pattern and timing of diversification of Cetartiodactyla (Mammalia, Laurasiatheria), as revealed by a comprehensive analysis of mitochondrial genomes. *C R Biol* **335**, 32–50.

Hillenius WJ (1992) The evolution of nasal turbinates and mammalian endothermy. *Paleobiology* **18**, 17–29.

Hillenius WJ (1994) Turbinates in therapsids: evidence for late Permian origins of mammalian endothermy. *Evolution* **48**, 207–229.

Janis CM (1990) Correlation of cranial and dental variables with dietary preferences in mammals: a comparison of macropodoids and ungulates. *Mem Queensland Mus* **28**, 349–366.

Laska M (2005) the number of functional olfactory receptor genes and the relative size of olfactory brain structures are poor predictors of olfactory discrimination performance with enantiomers. *Chem Senses* **30**, 171–175.

Mourlam MJ, Orliac MJ (2017) Infrasonic and ultrasonic hearing evolved after the emergence of modern whales. *Curr Biol* **27**, 1776–1781.

Orliac M, Boisserie J-R, MacLatchy L, et al. (2010) Early Miocene hippopotamids (Cetartiodactyla) constrain the phylogenetic and spatiotemporal settings of hippopotamid origin. *PNAS* **107**, 11871–11876.

Pihlström H (2008) Comparative anatomy and physiology of chemical senses in aquatic mammals. In: *Sensory Evolution on the Threshold: Adaptations in Secondarily Aquatic Vertebrates* (eds. Thewissen JGM, Nummela S), pp. 95–109. Berkeley: University of California Press.

Pihlström H (2012) The size of major mammalian sensory organs as measured from cranial characters, and their relation to the biology and evolution of mammals. *Diss Biocentri Viikki Univ Helsingiensis* **44**, 1–78.

Ranslow AN, Richter JP, Neuberger T, et al. (2014) Reconstruction and morphometric analysis of the nasal airway of the white-tailed deer (*Odocoileus virginianus*) and implications regarding respiratory and olfactory airflow. *Anat Rec* **297**, 2138–2147.

Reidenberg JS, Laitman JT (2008) Sisters of the sinuses: cetacean air sacs. *Anat Rec* **291**, 1389–1396.

Stromer E (1903) *Zeuglodon*-reste aus dem Oberen Mittlelocän des Fajum. *Beitr Paläont Österreich-Ungarns Orients* **15**, 65–100.

Thewissen JGM, Nummela S (2008) Sensory evolution in aquatic tetrapods: toward and integrative approach. In: *Sensory Evolution on the Threshold: Adaptations in Secondarily Aquatic Vertebrates* (eds Thewissen JGM, Nummela S), pp. 333–340. Berkeley: University of California Press.

Thewissen JGM, Cooper LN, Clementz MT, et al. (2007) Whales originated from aquatic artiodactyls in the Eocene epoch of India. *Nature* **450**, 1190–1194.

Uhen MD (2004) Form, function, and anatomy of *Dorudon atrox* (Mammalia, Cetacea): an Archaeocete from the Middle to Late Eocene of Egypt. *Univ Michigan Paleontol Papers* **34**, 1–222.

Uhen MD (2010) The Origin(s) of Whales. *Annu Rev Earth Planet Sci* **38**, 189–219.

Van Valkenburgh B, Theodor J, Friscia A, et al. (2004) Respiratory turbinates of canids and felids: a quantitative comparison. *J Zool* **264**, 281–293.

Van Valkenburgh B, Curtis A, Samuels JX, et al. (2011) Aquatic adaptations in the nose of carnivorans: evidence from the turbinates. *J Anat* **218**, 298–310.

Zachos J (2001) Trends, rhythms, and aberrations in global climate 65 Ma to Present. *Science* **292**, 686–693.

Zhou X, Xu S, Yang Y, et al. (2011) Phylogenomic analyses and improved resolution of Cetartiodactyla. *Mol Phylogenet Evol* **61**, 255–264.